ISSN: 2754-4753

Journal of Physics & Optics Sciences

SCIENTIFIC Research and Community

Research Article

Open Access

Design and Implementation of a Semi-Reflective Plate Operating in the Visible and near Infrared Fields, with Reflection Coefficient Robust to the Light Wavelength and Angle of Incidence

Mohammad Saeed Marouf

Head of the Laboratory of Laser Technology, And Faculty Member in the Higher Institute of Laser Researches & Applications (HILRA), Damascus University, Syria

ABSTRACT

This research illustrates the design of a parallel plate reflector operating in the visible and near infrared fields, with a reflection and/or transmission coefficients equal to 50%, and robust to the polarization of the used light and its extinction ratio (PER), in each of the two directions of polarization (perpendicular S and parallel P). Also there is no need for accurate adjustment of the plate so that the angle of incidence is exactly equal to 45°.

The research has its various applications in optical measurements laboratories, laser technology laboratories, optical communication laboratories, and photography.

One of the most important applications of this plate is ophthalmology devices, which can be used as glasses for people with impaired vision, light measurements in laser laboratories and optical measurements.

Purpose of the Research: The need for the use of one semi-reflector plate for all the visible and near infrared fields, instead of using one for each wavelength or light field, which will reduce the number of needed optical pieces used in the optical measurement and laser technology laboratories, because of its wide applications.

***Corresponding author**

Mohammad Saeed Marouf, Head of the Laboratory of Laser Technology, And Faculty Member in the Higher Institute of Laser Researches & Applications (HILRA), Damascus University, Syria, E-Mail: saeedmaroof123@gmail.com

Received: August 24, 2021; **Accepted:** August 30, 2021; **Published:** September 10, 2021

Introduction

In general, the semi-reflector plates operate in a specified wavelength of light each, and its efficiency is reduced when used for a wavelength other than the specified one, i.e the reflection and/or transmission coefficient varies. Also, the ratio of the reflected (and transmitted) light is different for the two different incident polarizations (perpendicular S and parallel P), and it needs a highly accurate adjustment of the angle of incidence to 45° for the proper work of the semi-reflector plate [1-5].

Traditional Methodology of Manufacturing

The traditional methodology of manufacturing reflector plates is based on coating of the semi-reflector plate for a one specified wavelength or more, and there is a need for a 45° adjustment of the angle of incidence to obtain a 50% reflection and/or transmission ratio of the incident light [2-7].

The Proposed Methodology

The proposed methodology is valid for any wavelength of the incident light, and there is no adjustment needed for the reflector plate to 45°, as it is effective whatever is the value of the incidence angle.

In this work, the manufacturing of a semi-reflector plate has been achieved, which can be used for all wavelengths in the visible and near infrared fields, via reflecting 50% of the incident light in terms of energy, and transmitting the other 50% [8-11].

Research Approach

The research work involves the following essential steps:

1. Design of the parallel plate reflector.
2. Coating of the parallel plate reflector.
3. Measurements and tests of the parallel plate reflector using various types of continuous lasers with different wavelengths, and high precision power meter.
4. Conclusion and Discussion.

Design of the Parallel Plate Reflector

The design of the parallel plate reflector has been done using the advanced design software "Zemax", and the optical lightning chart has been drawn. The chart illustrates the optical and surface quality requirements during the manufacturing process, such as the type of the used optical glass free from cracks, air bubbles, and all other optical defects in the glass structure that causes refraction and absorption of the light passing it, which in turn results in light

loss of power. The chart also illustrates the allowed number of newton rings N = 0.3 ΔN = 0.1, the null light absorption of the used glass, and the parallelism precision between the two parallel plate's surfaces of no more than 2". The optical diameter of the plate is 85 mm, and its thickness is 8 mm, and must be coated with anti-reflective coating suitable for the visible and near infrared field (ARC), to get rid of Fresnel reflection. Figure (1) shows the optical chart of a parallel plate reflector designed according to the Russian Гост optical standard, where the used optical glass is BK7, coated with chess squares of chrome light-reflective coating.

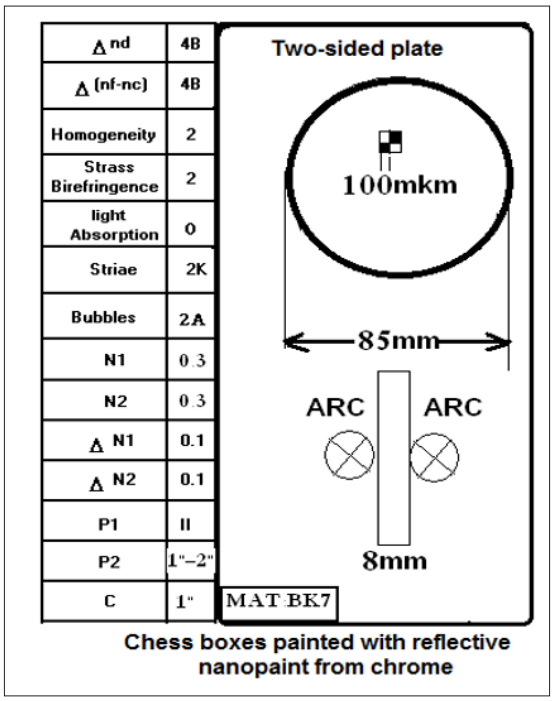

Figure 1: the optical chart of a parallel plate reflector of BK7 glass coated with chess squares of chrome light-reflective coating.

Figure (2-a) shows the parallel plate reflector with the interference fringes of the optical surface. The figure also shows the precision manufacturing specification ΔN = λ/4, surface flatness parameter N < 0.3, and the equatorial parameter ΔN < 0.1 [12-14].

The measurements have been done using the Fizeau Interferometer device shown in figure (2-b)

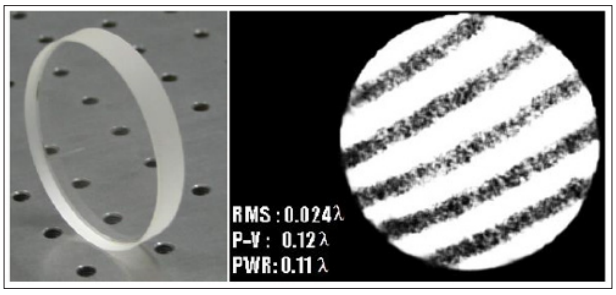

Figure (2-a): The parallel plate reflector with the interference fringes of the optical surface. ΔN=λ/4

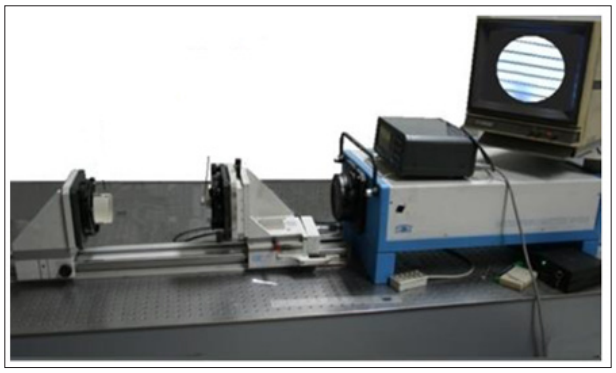

Figure (2-b): Fizeau Interferometer device

Coating

After manufacturing of the semi reflective parallel plate, it is cleaned properly in a white room, and then tested for light transmission and the other optical parameters' measurements, such as the precision manufacturing specification and parallelism precision. After that, the optical surfaces are re-cleaned to ensure the properness of the next coating process.

Through the coating process, the plate is first coated on the two faces with an anti-reflective coating suitable for the visible and near infrared fields (ARC), to get rid of Fresnel reflection, so that it could maintain the required values of reflection and/or transmission coefficients, of 50% each, and then re-coated with many layers of chrome 100% reflective coating using the thin films method. Next, the coating is removed from half of the plate's surface in a chess-like shape with equal micro-dimensions squares of 100μm x100μm. In this way, the plate will totally reflect the light on half of its surface through the chrome 100% reflective coated windows, while it totally transmits the light through the other uncoated half. That is, the reflection and/or transmission coefficients are equally 50% of the incident light each, and the semi reflective plate is thus achieved. It is worth noting that in the case of mirror reflection, regardless whether the light is polarized or not, and whatever is the type of polarization (perpendicular S or parallel P), it is reflected in the same manner and in the same amount for all wavelengths according to an incidence angle equal to reflection angle (Snell's law). That is, it is no matter for the incidence angle to be exactly 45°, as it is clear in the chart shown in figure (3-a). Figure (3-b) shows the digital image of this semi reflective plate called Polka Plate [15-18].

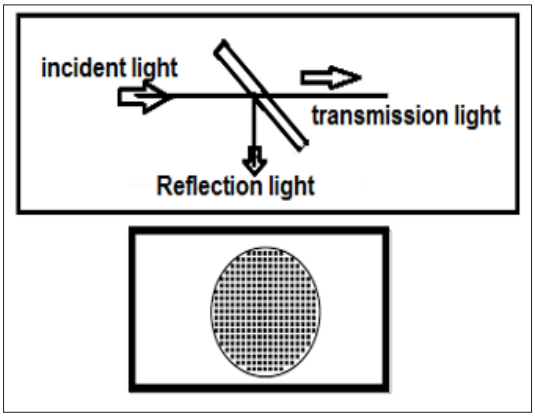

Figure (3-a): Measurement method of reflected and transmitted light through the semi reflective plate after chess-like coating (Polka Plate).

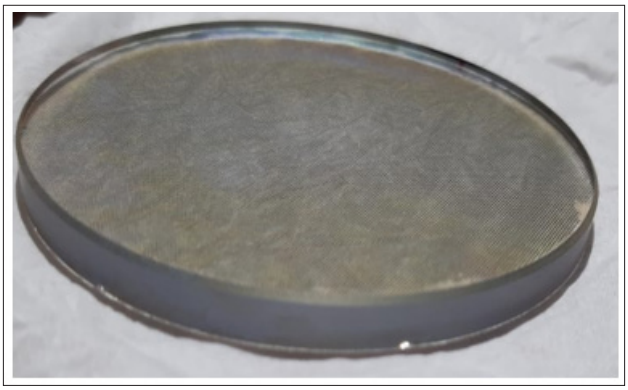

Figure (3-b): Horizontal image of the semi reflective plate after coating showing the thickness and the deposit of the chess-like coating

Figure (3-C): A digital image of the half-reflective plate of light after chess paint, Fresnel reflection coating and vertical positioning method.

Measurements

Measurements have been conducted by various continuous lasers of different wavelengths, using a high precision power meter, and taking into account the light noise, as it is shown in figure (4) [16-18]. Figure (5) shows a real image of the mentioned semi reflective plate during testing, using a Gaussian homogenous (He-Ne) laser light of 632.8 nm wavelength.

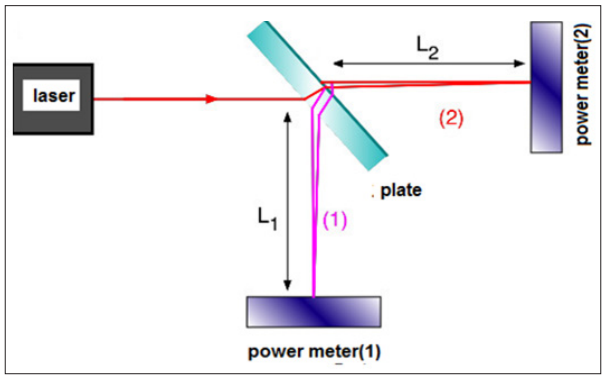

Figure 4: Test method of the semi reflective plate using high precision power meter

Figure 5: Real image of the semi reflective plate during testing.

The following table (table 1) shows the conducted measurements using different wavelengths of various lasers in the visible and near infrared fields, which represents the most used lasers in the optical and communication measurements and applications. These are:

- Blue laser diode of 445 nm wavelength.
- He-Ne laser of 632.8 nm wavelength.
- First harmony ND-YAG of 1064 nm wavelength.
- Second harmony ND-YAG of 532 nm wavelength.
- Red laser diode of 650 nm wavelength.
- Adjusted power, near infrared laser diode of 808 nm wavelength.

The conducted measurements include measurements of the incident light before the plate, the reflected light from the plate, and the transmitted light through it. Also taken into account in these measurements, as it is shown in table 1, is the light noise, whose power SN doesn't exceed 50 µw, which is a low power value comparing with that for the signal of laser light source. Light dampers have been used to make the power level of all used lasers close to each other.

Table 1: Test measurements of the parallel plate reflector for different wavelengths

The type of laser used	Wavelengths λ(nm)	Total power P(mw)	Refection power p1	Transmitted power p2	Optical noise N
He-Ne laser	632.8nm	2.36mw	1.17	1.18	50µw
ND:YAG laser	1.064nm	5mw	2.54	2.4	50µw
(ND:YAG) SHG	532nm	5mw	2.55	2.50	50µw
Laser Diode	650nm	2.86mw	1.44	1.42	50µw
Laser Diode	808nm	10mw	5.18	5.1	50µw
Laser Diode	445nm	5mw	2.55	2.50	50µw

The light detectors used in the power and noise measurements are of high precision coherent type, having a resolution of 0.5 µw. The measured signal to noise ratio is:

S/N = Log (2500/50) = 3.92

The value above is for low power lasers in the rank of 2.5 mw. For moderate and high power lasers, the noise power measurement is negligible. Figure (6) shows Measuring laser optical noise with Coherent light detector.

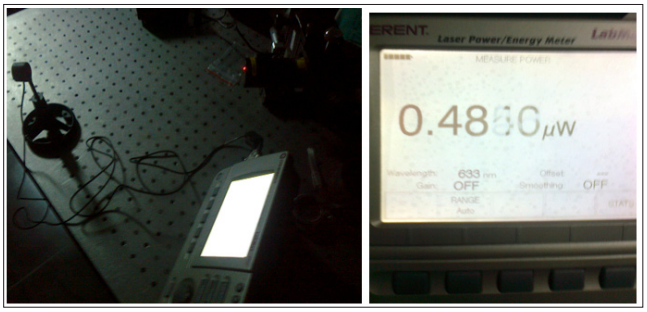

Figure 6: shows Measuring laser optical noise with Coherent light detector

Figure (7) shows the curves for the percentage of light for each of the reflected and transmitted beam at different wavelengths, and for different incidence angles. In these curves the vertical axis represents the percentage of light, and the horizontal axis represents the wavelengths for the lasers used in the experiment. As it is shown, the difference doesn't exceed 1% between the two beams at different incidence angles. That is, unlike the traditional parallel plate reflectors and cubic beam splitters, the percentage is the same whatever is the incidence angle, and regardless whether it is exactly equal to 45° or not. This result is very important especially as it is very hard to adjust the incidence angle in the laboratory tests.

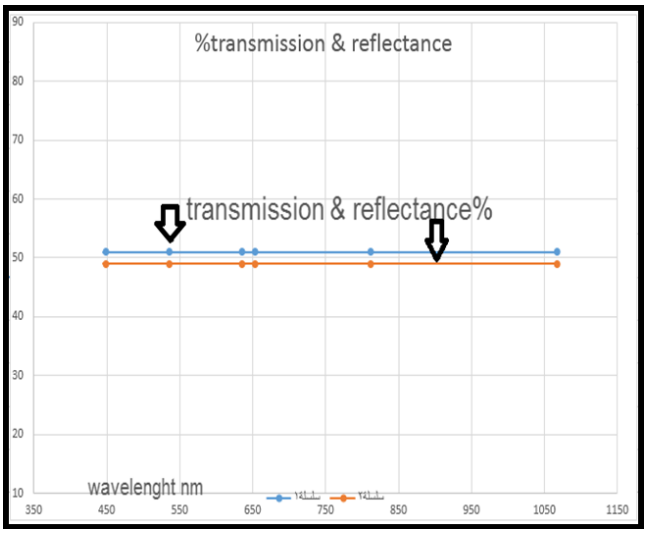

Figure 7: The curve for the percentage of light for each of the reflected and transmitted beam. The upper curve is for the transmitted light, and the lower is for reflected light

Conclusion and Discussion

In this work, a semi reflective parallel plate, that can be used for all wavelengths in the visible and near infrared fields, has been achieved. The plate transmits half of the light power, and reflect the other half in the visible and near infrared fields. It has been proven by test that, unlike the traditional parallel plate reflectors and cubic beam splitters, the difference between the percentage of transmitted light and the that of reflected light doesn't exceed 1%, whatever is the incidence angle, and regardless whether it is exactly equal to 45° or not. This result is very important especially as it is very hard to adjust the incidence angle in the laboratory tests. The designed plate is better than many other types of reflectors because of its low cost and wide applications in the visible and near infrared fields.

Applications for this Work

One of the most important applications of this plate is ophthalmology devices, which can be used as glasses for people with impaired vision, light measurements in laser laboratories and optical measurements.

Data Availability

The detailed experimental data used to support the findings of this study is available from the corresponding author upon request

https://orcid.org/0000-0003-2657-1605

References

1. Pace DP, Kenney KL, Galiher DL (2002) Laser assisted arc welding of ultra-high strength steels. Proc 6th- Trends in Welding Research, Pine Mountain, GA 442-447-p.
2. McPherson NA (2006) "Thin plate distortion reduction—a management or technology issue?" Welding and Cutting 5: 277-282.
3. Roland F, Manzon L, Kujala P, Brede M, Weitzenböck J (2004) Advanced joining techniques in European Shipbuilding. Journal of Ship Production 20: 200-210.
4. Sa´nchez-Amaya JM, Delgado T, Gonza´ lez Rovira L, Botana FJ (2009) Laser welding of aluminium alloys 5083 and 6082 under conduction regime. Applied Surface Science 255: 9512-9521.
5. Park, S. H. C., Sato, Y. S., Kokawa, H.; 161. "Effect of micro-texture on fracture location in friction stir weld of Mg alloy AZ61 during tensile test. Scripta Materialia 49: 161-166.
6. Thomas WM, Nicholas ED (1997) Friction stir welding for the transportation industries. Mater Des 18: 269-273.
7. Thomas WM, Nicholas ED, Needham JC, Murch MG, Dawes CJ (1991) Friction stir butt welding. International Patent, PCT/GB92/02203.
8. Reynolds AP, Tang W, Posada M, DeLoach J (2013) Friction stir welding of DH36 steel. Science and Technology of Welding and Joining 8: 455-461.
9. Lienert TJ, Tang W, Hogeboom JA, Kvidahl LG (2003) Friction stir welding of DH36 steel. Proceedings of 4th International Symposium on Friction Stir Welding, May 14-16, 2003, Park City, UT.
10. Barnes SJ, Steuwer A, Mahawish S, Johnson R, Withers PJ (2008) Residual strains and microstructure development in single and sequential double sided friction stir welds in RQT-701 steel. Materials Science and Engineering A 492: 35-44.
11. Su JQ, Nelson TW, Mishra R, Mahoney M (2003) Microstructural investigation of friction stir welded 7050-T651 aluminium. Acta Materialia 51: 713-729.
12. Lancaster JF (1999) Metallurgy of welding - Sixth Edition. Abington Publishing 464-465-p.
13. Cook G, Nielsen B (2007) An Analytical Solution to Heat Dissipation during Friction Stir Welding of Steel X65. JAMHT 1: 1-13.
14. Buffa G, Fratini L, Pasta S, Shivpuri R (2008) On the thermo-mechanical loads and the resultant residual stresses in friction stir processing operations. CIRP Annalsys Manufacturing Technology 57: 287-290.
15. Bao S, Zhao G, Yu C, Chang Q, Ye C, et al. (2011) Recrystallization behavior of a Nb-microalloyed steel during hot compression. Applied Mathematical Modelling 35: 3268-3275.

16. Liang-yun L, Chun-lin Q, De-wen Z, Xiu-hua G, Lin-xiu D (2011) Dynamic and Static Recrystallization Behavior of Low Carbon High Niobium Microalloyed Steel. Journal Of Iron And Steel Research 18: 55-60.
17. Mejía I, Bedolla-Jacuinde A, Maldonado C, Cabrera JM (2011) Determination of the critical conditions for the initiation of dynamic recrystallization in boron microalloyed steels. Materials Science and Engineering A 528: 4133-4140.
18. Mirzadeh H, Cabrera JM, Prado JM, Najafizadeh A (2011) Hot deformation behavior of a medium carbon microalloyed steel. Materials Science and Engineering A 528: 3876-3882.